applied sciences

MDPI

Article

Unveiling the Influence of Carbon Nanotube Diameter and Surface Modification on the Anchorage of L-Asparaginase

Raquel O. Cristóvão [1,2,*], Rita A. M. Barros [1,2], João G. Pinho [1,2], Lília S. Teixeira [1,2], Márcia C. Neves [3], Mara G. Freire [3], Joaquim L. Faria [1,2], Valéria C. Santos-Ebinuma [4], Ana P. M. Tavares [3,*] and Cláudia G. Silva [1,2]

1 LSRE-LCM—Laboratory of Separation and Reaction Engineering-Laboratory of Catalysis and Materials, Faculty of Engineering, University of Porto, Rua Doutor Roberto Frias, 4200-465 Porto, Portugal
2 ALiCE—Associate Laboratory in Chemical Engineering, Faculty of Engineering, University of Porto, Rua Doutor Roberto Frias, 4200-465 Porto, Portugal
3 CICECO—Aveiro Institute of Materials, Department of Chemistry, University of Aveiro, 3810-193 Aveiro, Portugal
4 Department of Bioprocess Engineering and Biotechnology, School of Pharmaceutical Sciences, São Paulo State University (UNESP), Araraquara 14800-903, São Paulo, Brazil
* Correspondence: roc@fe.up.pt (R.O.C.); aptavares@ua.pt (A.P.M.T.); Tel.: +351-220-413-658 (R.O.C.); +351-234-401-520 (A.P.M.T.)

Abstract: L-asparaginase (ASNase, EC 3.5.1.1) is an amidohydrolase enzyme known for its anti-cancer properties, with an ever-increasing commercial value. Immobilization has been studied to improve the enzyme's efficiency, enabling its recovery and reuse, enhancing its stability and half-life time. In this work, the effect of pH, contact time and enzyme concentration during the ASNase physical adsorption onto pristine and functionalized multi-walled carbon nanotubes (MWCNTs and f-MWCNTs, respectively) with different size diameters was investigated by maximizing ASNase relative recovered activity (*RRA*) and immobilization yield (*IY*). Immobilized ASNase reusability and kinetic parameters were also evaluated. The ASNase immobilization onto f-MWCNTs offered higher loading capacities, enhanced reusability, and improved enzyme affinity to the substrate, attaining *RRA* and *IY* of 100 and 99%, respectively, at the best immobilization conditions (0.4 mg/mL of ASNase, pH 8, 30 min of contact time). In addition, MWCNTs diameter proved to play a critical role in determining the enzyme binding affinity, as evidenced by the best results attained with f-MWCNTs with diameters of 10–20 nm and 20–40 nm. This study provided essential information on the impact of MWCNTs diameter and their surface functionalization on ASNase efficiency, which may be helpful for the development of innovative biomedical devices or food pre-treatment solutions.

Keywords: L-asparaginase; carbon nanotubes diameter and functionalization; enzyme immobilization

Citation: Cristóvão, R.O.; Barros, R.A.M.; Pinho, J.G.; Teixeira, L.S.; Neves, M.C.; Freire, M.G.; Faria, J.L.; Santos-Ebinuma, V.C.; Tavares, A.P.M.; Silva, C.G. Unveiling the Influence of Carbon Nanotube Diameter and Surface Modification on the Anchorage of L-Asparaginase. *Appl. Sci.* **2022**, *12*, 8924. https://doi.org/10.3390/app12178924

Academic Editor: Marilena Carbone

Received: 26 July 2022
Accepted: 1 September 2022
Published: 5 September 2022

1. Introduction

Recently, interest in the production of biopharmaceuticals has grown due to their high sensitivity, specificity, low risk and adverse effects for the patient [1]. Biopharmaceuticals are mostly therapeutic recombinant proteins obtained by biotechnological processes [2]. L-asparaginase (ASNase) (EC 3.5.1.1) is an example of a biopharmaceutical with extensive use in the treatment of acute lymphoblastic leukemia (ALL), which is the most frequent type of leukemia in children up to 14 years old [3]. ASNase circulates in the blood system for only a short time before being hydrolyzed by native proteases. This property can lead to a restriction of enzyme effectiveness. They are also primarily unstable and thermolabile enzymes. Therefore, to prolong its lifetime, reduce its potential side effects, and enhance drug effects in blood, the native ASNase is often immobilized on various supports. It is reported that this process can reduce immunity, toxicity and improve the resistance to proteolysis [4]. The commercial approved PEG-asparaginase is an example of a confined

enzyme obtained from an *Escherichia coli*-derived ASNase that is subsequently covalently linked to polyethylene glycol. It is reported to cause 18% of hypersensitivity reactions, compared with 32% for native ASNase [5].

ASNase application in the food industry is also very relevant since it can promote acrylamide mitigation without flavor changes. Acrylamide is considered a probable carcinogen to humans, formed by Maillard reaction between L-asparagine and reducing sugars of starchy foods [6]. Nevertheless, ASNase must be more stable during all the processing steps in the food industry.

ASNase immobilization is a technique that can overcome the hindrances of its application in the pharmaceutical and food industries, increasing enzyme stability and half-life without activity loss [6]. Over the last twenty years, carbon-based nanomaterials, such as carbon nanotubes (CNTs), have started to be used to immobilize enzymes [5,7,8]. CNTs are carbon allotropes constituted by sheets of graphene with cylinder form. When multiple concentric graphitic tubes are wrapped around a single axis, they are designated multi-walled carbon nanotubes (MWCNT). CNTs have excellent mechanical, chemical, optical, and electrical properties, presenting a high loading capacity [7,9]. These characteristics, together with their biocompatibility, makes CNTs appropriate nanomaterials for the use in the pharmaceutical industry [10,11]. Additionally, CNTs' surface can be easily functionalized, tuning their properties towards precise applications and improving their efficacy as enzymes support [12].

Immobilizing biomolecules onto CNTs can be carried out by different methods, explicitly non-covalent processes, such as direct physical adsorption, physical adsorption onto CNTs functionalized with biomolecules, polymers, or surfactants and layer-by-layer deposition, and covalent attachment, either with or without crosslinkers [13–15]. Adsorption is the preferred method for enzyme immobilization onto CNTs since it is a conservative and straightforward method concerning the conformational structure of the biomolecules and CNTs properties [16]. However, the main disadvantage of this method concerns the detachment of the biomolecules from the CNTs surface [17]. This can be battled by CNTs functionalization by introducing different surface groups such as carboxyl, amine, glycol, among others [18,19]. Moreover, the surface modification increases the CNTs' compatibility with biomolecules, such as enzymes, by permanent or reversible modifications that change their chemical properties [4]. Although promising results using modified CNTs can be found, only a few works reporting the immobilization of ASNase onto functionalized CNTs are published [20,21]. Studies on MCWNTs still lack key parameters, such as their structure, size, surface chemistry, charge, and shape, determinant for the nanomaterials' biocompatibility.

In previous works, we studied the ASNase adsorption onto pristine [9] and oxidized MWCNTs with a specific diameter [22]. To fully explore the enzyme-CNT complex potential, it is essential to also find the optimal diameter for CNTs. Zhao et al. [23] found that adsorbed bovine serum albumin (BSA) stability is determined by the diameter and surface area of CNTs. Mu et al. [24] also reported a selective protein (BSA, carbonic anhydrase, hexokinase) binding depending on the protein and MWCNTs diameter. In this work, the immobilization of commercial ASNase was studied for the first time onto pristine and f-MWCNTs with different diameter ranges (from <10 to 100 nm). The wide range of diameters tested, together with the functionalization of the MWCNTs surface, are key for the novelty of this work and represent a step forward in the study of enzyme's immobilization over nanomaterials. Two important MWCNTs characteristics were evaluated: the specific surface area and pH of the point of zero charge (pH_{PZC}), along with the determination of the ASNase isoelectric point (pI). The adsorption conditions such as contact time, medium pH and ASNase concentration were also improved to reach the maximum RRA of immobilized enzyme and IY. Finally, the ASNase-MWCNT complex was characterized in terms of kinetic properties and operational stability.

2. Materials and Methods

2.1. Materials, Enzyme and Chemicals

Deltaclon S.L., Spain, provided *E. coli* ASNase type II (>96% purity) 10,000 IU lyophilized with no additives and with 269 IU/mg (ENZ-287) specific activity. Pristine MWCNTs of different outside diameter ranges were purchased from NTP Shenzhen Nanotechnologies Co., Ltd. (Shenzhen, China), presenting the manufacture advertised characteristics shown in Table 1. L-Asparagine (≥99.0%), tris (hydroxymethyl) aminomethane (TRIS) (≥99.0%) and disodium hydrogen phosphate (≥99.0%) were supplied by VWR International, LLC. Trichloroacetic acid (TCA) (≥99.0%) was purchased from J.T. Baker. Citric acid (≥99.5%) and Nessler's reagent (dipotassium tetraiodomercurate (II)) were obtained from Merck Chemical Company (Darmstadt, Germany). Sodium hydroxide (≥98.0%) and hydrochloric acid (37%) were provided by Sigma-Aldrich (St. Louis, MO, USA).

Table 1. Multi-walled carbon nanotubes (MWCNTs) physical properties according to manufacturer data.

Base Material	Diameter Range (nm)	Length (μm)	Purity (%)	Ash (wt %)	Specific Surface Area Range (m^2/g)
MWCNT-10	<10	>5	>97	<3	250–500
MWCNT-1020	10–20	>5	>97	<3	100–160
MWCNT-2040	20–40	>5	>97	<3	80–140
MWCNT-60100	60–100	>5	>97	<3	40–70

2.2. Characterization Techniques

The Brunauer-Emmett-Teller (BET) specific surface area (S_{BET}) of every type of MWCNTs used was calculated using the N_2 adsorption data at −196 °C in the relative pressure range 0.05–0.20 by means of a Quantachrome NOVA 4200e apparatus. The pH_{PZC} of the MWCNT samples was determined using a drift method described elsewhere [25].

2.3. Determination of ASNase Isoelectric Point

The *pI* of ASNase was determined by measuring the zeta potential of aqueous solutions of ASNase (0.086 mg/mL) in a wide range of pH values. Aqueous solutions of NaOH and HCl 0.01 M were used to adjust the pH. The results were acquired by the equipment Malvern Zetasizer Nano ZS (Malvern Instruments Ltd., Malvern, United Kingdom) at room temperature (25 °C) and using an appropriate cell to perform this experiment. The zeta potential was read at least 20 times, and the test was performed in triplicate.

2.4. MWCNTs Functionalization

Hydrothermal oxidation of the pristine MWCNTs was performed in a Teflon-lined stainless-steel autoclave using 0.5 M HNO_3 aqueous solutions at 200 °C, as described elsewhere [26]. Briefly, 0.2 g of MWCNTs was added to 75 mL of an HNO_3 aqueous solution. After being sealed, the vessel was put into an oven at 200 °C for 2 h. Then, the MWCNTs were recovered, rinsed with water until neutral, and dried overnight at 120 °C.

2.5. ASNase Immobilization over MWCNT

The ASNase immobilization by physical adsorption onto different MWCNTs was investigated according to the procedure described elsewhere [27] by combining 2 mg of each material with 200 μL of several ASNase solution concentrations, ranging from 0.05 to 0.7 mg/mL (ASNase activity ranging from 4 to 9.5 U/mL) in a suitable buffer. The pH value was varied using different buffers: citrate-phosphate buffer for pH 4.0, phosphate buffer for pH 6.0 and 8.0 and carbonate-bicarbonate buffer for pH 9.0. Immobilization was achieved by swirling the mixtures in a multifunctional tube rotator (Grant Instruments Lda., model PTR-35) for a set amount of time and then the samples were centrifuged at 112× *g* using a MicroStar 12 VWR centrifuge for 10 min to separate the MWCNTs from the supernatant. The contact time was improved at the selected best pH by immobilizing

during different periods (30, 60, 120 min). At the same time, control was made with free ASNase under the studied conditions. For each assay, duplicate runs were made.

2.6. ASNase Activity Measurement

According to the procedure used in previous studies of the research group [9], the ASNase activity was evaluated by measuring the amount of ammonia produced after L-asparagine (substrate) hydrolysis. The experimental method involves the stirring for 30 min at 37 °C of 50 µL of L-asparagine (189 mM) with 50 µL of ASNase solution (initial free enzyme or supernatant after immobilization) or with 2.0 mg of ASNase adsorbed on MWCNTs (immobilized enzyme) in 500 µL of TRIS-HCl buffer (50 mM, pH 8.6), and 450 µL of deionized water. After incubation, the reaction was stopped by adding 250 µL of TCA 1.5 M to the free enzyme, while the supernatant was removed from the immobilized one. The amount of generated ammonia was then measured by mixing 100 µL of the prior free ASNase solution or supernatant with 2.15 mL of deionized water and 250 µL of Nessler's reagent. The rise in absorbance was measured during 30 min at 436 nm, using a JASCO V-560 UV-Vis spectrophotometer at room temperature. Ammonium sulfate was used to establish a calibration curve.

The determination of free and immobilized ASNase activity, as well as the determination of the immobilization yield (*IY*) and of the relative recovered activity (*RRA*) of the immobilized enzyme are defined by Equations (S1)–(S4), respectively, in the supporting information.

2.7. Operational Stability of Immobilized ASNase

The operational stability of immobilized ASNase was evaluated by incubating 2 mg of the ASNase-MWCNT bioconjugate with 50 µL of L-asparagine (189 mM) in 500 µL of TRIS-HCl buffer (50 mM, pH 8.6), and 450 µL of deionized water at 37 °C under stirring. The reaction was halted after 30 min of each cycle by removing the supernatant and adding 250 µL of TCA 1.5 M. To start the next cycle, the bioconjugate was washed twice with phosphate buffer pH 7.0 (±500 µL per wash) and resuspended in a fresh L-asparagine solution. Six cycles of operational stability testing were performed, with triplicate runs for each experiment.

2.8. Enzymatic Kinetic Parameters

The Hill Equation (Equation (1)) was used to evaluate the kinetic behavior of free and immobilized ASNase:

$$v = \frac{v_{max}[S]^n}{S_{50}^n + [S]^n} \quad (1)$$

where S_{50} is the substrate concentration (S) at which the initial reaction rate (v) is equal to 50% of the maximum reaction rate (v_{max}) and n is the Hill coefficient.

The ASNase activity was measured using L-asparagine as substrate throughout a 0.5–750 mM range of initial concentrations to determine the kinetic parameters S_{50}, v_{max} and n. The parameter values were acquired using CurveExpert software to fit a nonlinear curve to the reaction rate vs. L-asparagine concentration plot. The ratio of k_{cat} (turnover number) to S_{50} was used to evaluate the ASNase efficiency, while k_{cat} was determined by dividing v_{max} by the total concentration of ASNase [28].

3. Results and Discussion

3.1. Characterization of MWCNTs

CNTs have been reported as adequate support for enzymes immobilization, mainly due to their high specific surface area and high enzyme loading capacity [29–31]. Additionally, CNTs' surface can be easily functionalized, tuning their properties towards specific applications, and enhancing their efficiency as enzyme support. In this way, the pristine MWCNTs were oxidized with HNO_3 (0.5 M) in order to generate materials with large amounts of surface oxygen groups, namely carboxylic acids, anhydrides, quinones,

or phenols [30]. Two important characteristics of the support to the immobilization of enzymes are the pH_{PZC}, i.e., the pH at which the net charge of total particle surface is equal to zero, and the S_{BET}. The pH_{PZC} of the pristine MWCNTs was determined using a drift method, being the value around 7, a value close to other CNTs reported in the literature (7.3) [32]. The introduction of acid groups on the surface through oxidation of pristine MWCNTs lead to a pH_{PZC} of f-MWCNTs around values of 3–4.

The S_{BET} of pristine and f-MWCNTs determined by the BET method through N_2 adsorption-desorption isotherms are displayed in Table 2. As the MWCNTs diameter increases, there is a decrease in their surface area, as reported by Pigney et al. [33] and Chen et al. [34]. On the other hand, the hydrothermal oxidation treatment led to an increase in the surface area of MWCNTs, explained by the creation of defects on the MWCNTs sidewalls along with the opening of the MWCNTs end caps, causing an increase in the porosity [15]. These additional apertures allow access to the MWCNTs cavity, increasing S_{BET}. According to Silva et al. [15], this type of materials functionalization produces MWCNTs mainly with carboxylic acid (-COOH) surface groups. Therefore, an acidity increase in the MWCNTs surface and a decrease in pH_{PZC} to lower values is expected after treatment with HNO_3.

Table 2. Brunauer-Emmett-Teller specific surface area (S_{BET}) of pristine and functionalized multi-walled carbon nanotubes.

	S_{BET} ($\pm$5 m^2/g)	
	MWCNT	**F-MWCNT**
MWCNT-10	350	408
MWCNT-1020	104	123
MWCNT-2040	67	85
MWCNT-60100	30	33

An easy separation from the aqueous solution is an intuitive advantage for protein immobilization. However, after centrifugation, some pristine MWCNTs, especially those with diameters of 20–40 nm and 60–100 nm, tended to remain in solution, hindering the separation process. This occurrence can be explained by the extreme hydrophobic characteristics of pristine MWCNTs with high diameters that may cause their aggregation [35]. f-MWCNTs demonstrated a more effortless and faster separation by centrifugation, as their different functional groups contributed to a decrease in hydrophobicity [36].

3.2. Determination of ASNase Isoelectric Point

The *pI* is the pH of a solution at which the net charge of the enzyme becomes zero. Thus, the *pI* determination allows verifying the enzyme charge at a given pH value, an important parameter for the enzyme's immobilization. When the solution pH value is equal to *pI*, the enzyme shows an absence of inter-particle repulsive forces, being the enzyme more compact and hydrophobic and, consequently, less soluble and stable [37]. Thus, the *pI* determination by isoelectric precipitation consists in varying the pH of a highly concentrated solution until protein precipitation. The knowledge of ASNase *pI* and MWCNTs pH_{PZC} is fundamental for understanding the type and forces of interaction between the support and the enzyme after immobilization [13].

The accession number in the UniProt database of the commercial ASNase from *E. coli* used in this work is P00805, meaning that it has about 348 amino acids and a mass of 139 kDa. The corresponding protein accession number was transferred to the ExPASy ProtPram tool, which estimated that the ASNase theoretical *pI* is around 5.66. However, this estimate may have some errors associated with ASNase quaternary structure and the probable methylation, deamidation reported [38] and post-translational modifications not accounted for in the ProtPram model used. Several authors reported an ASNase *pI* of 4.9 [39,40], ranging between 4.6 and 5.1, accounting for different mutations [41], which is somewhat different from the estimated theoretical *pI*.

In this work, the ASNase *pI* was determined using a method based on zeta potential, where the enzyme *pI* corresponds to the pH value where the zeta potential equals zero [37]. Figure 1 shows that the ASNase *pI* is around 5.2, close to the values reported in the literature [42]. The slight differences can be explained using different methods or ionic environments, such as ionic strength and ion type [37].

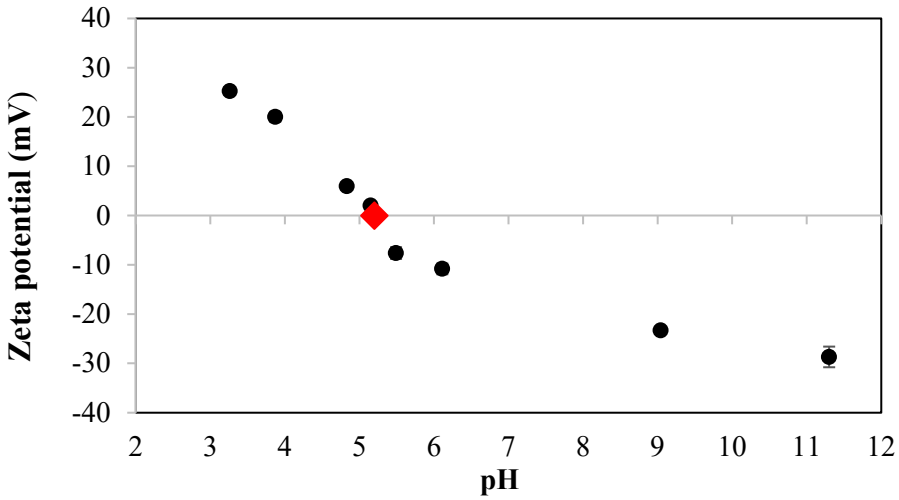

Figure 1. L-asparaginase (ASNase) zeta potential values for different pH values. ● Experimental data; ♦ isoelectric point.

3.3. Effect of pH on ASNase Immobilization onto MWCNTs

The immobilization of commercial ASNase was studied through physical adsorption onto MWCNTs and f-MWCNTs. The first parameter to be evaluated was the pH of the immobilization medium. The enzyme immobilization onto support is expected to be influenced by pH since it determines the protein and the MWCNTs' superficial charges and, consequently, the affinity or repulsion between them [13]. However, it must be considered that, at specific pH values, the enzyme may exhibit low activity or even be denatured, making the results inviable. This way, the immobilization of 0.086 mg/mL of ASNase onto 2 mg of both pristine and f-MWCNTs during 60 min was tested at different pH values (4, 6, 8 and 9). A control experiment with MWCNTs without enzyme was also performed, and no reaction or interference was detected in the enzyme activity method. According to Figure 2, the highest *RRA* of immobilized ASNase occurred at pH 8 for almost all the MWCNTs tested. Similar results were obtained by Noma et al. [42] during the immobilization of ASNase on tannic acid-modified magnetic mesoporous particles. It was also possible to verify that the ASNase immobilized onto f-MWCNTs showed higher *RRA* than when immobilized onto pristine MWCNTs with the same diameters and pH values. This result can be explained by the larger specific surface areas available for ASNase adsorption and the higher hydrophilicity of f-MWCNTs, which increases their dispersibility in aqueous medium and therefore the availability of adsorption sites.

The efficacy of the immobilization should be analyzed through a balance between the enzyme *RRA* and the *IY* results. Nevertheless, similar *IY* values were noticed for almost all the conditions studied, attaining above 90% (Figure S1 in the Supporting Information), which corresponds to almost total ASNase adsorption onto MWCNTs.

Considering that the *pI* of ASNase is 5.2 and the pH_{PZC} of pristine and f-MWCNTs is around 7 and 3, respectively, at pH $\geq$ 8, where the highest *RRA* were obtained, both enzyme and support surfaces are negatively charged. Thus, it is possible to conclude that electrostatic interactions do not seem to be the main driving force for the immobilization of ASNase under the tested conditions. Other interactions such as π-π interactions, CH-π interactions and hydrophobic interactions can be the cause of adsorption between MWCNTs/f-MWCNTs and ASNase [17].

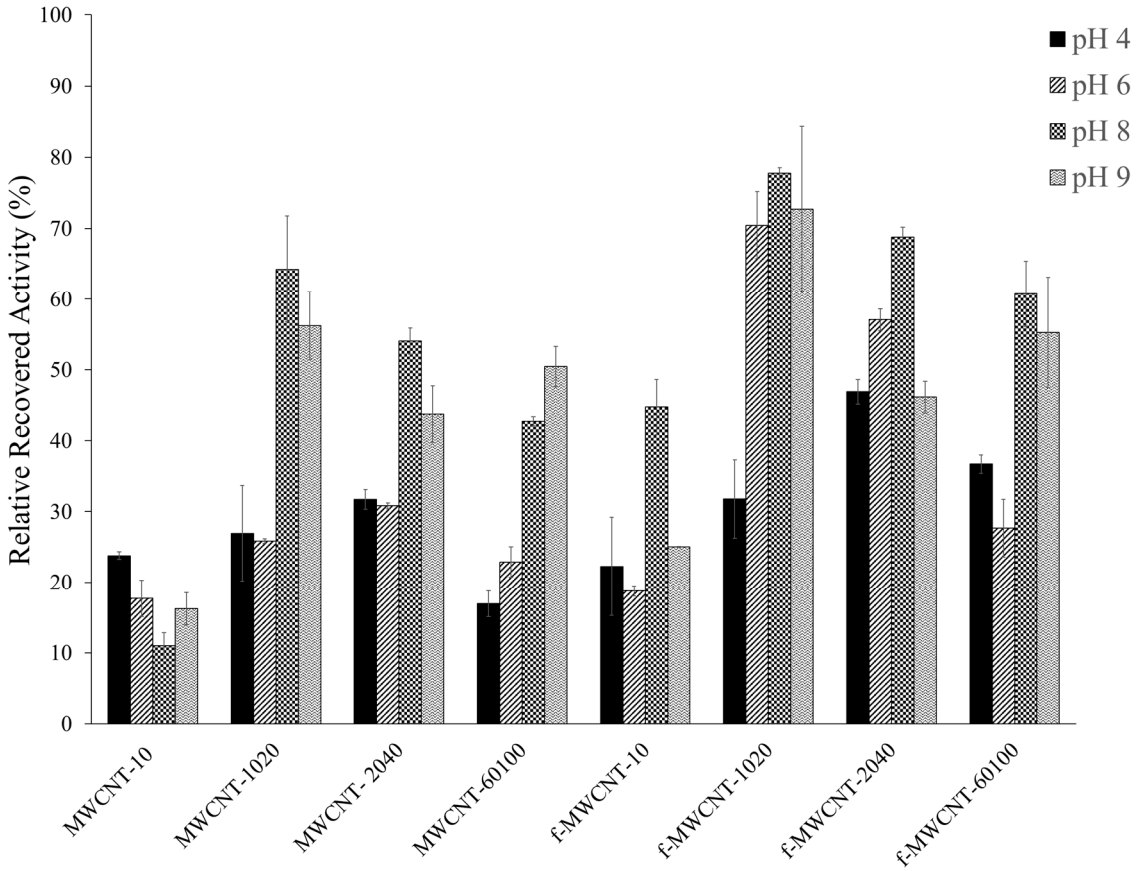

Figure 2. Effect of pH and diameter of multi-walled carbon nanotubes (MWCNTs) on the relative recovered activity (*RRA*). Immobilization of 0.086 mg/mL of L-asparaginase (ASNase) onto 2 mg of pristine multi-walled carbon nanotubes (MWCNTs) and functionalized MWCNTs (f-MWCNTs) for 60 min of contact time. Error bars correspond to the standard deviation between replicates.

The MWCNTs that displayed the best *RRA* (around 80%) were the f-MWCNT-1020, revealing that they have the adequate diameter (10–20 nm) and specific surface area to maintain the ASNase activity after immobilization as much as possible. Although MWCNT-10 have a higher specific surface area leading to *IY* values above 97% (Figure S1 in the Supporting Information), their diameter seems to be too small to keep all the enzyme molecules active. This correlation indicates that the surface area of the MWCNTs is an important parameter during the ASNase immobilization, but MWCNTs need to have an adequate diameter so that the adsorbed enzymes have their active sites available to react with the substrate.

3.4. Effect of Contact Time on ASNase Immobilization onto MWCNTs

To attain the maximum *IY* and *RRA* values, we assessed the influence of immobilization contact time. The adsorption of 0.086 mg/mL of ASNase onto 2 mg of MWCNTs/f-MWCNTs was evaluated for three different contact times (30, 60 and 120 min) and at pH 8 (best immobilization pH for most materials). The results of the effect of the immobilization time on the *RRA* are displayed in Figure 3, where it is possible to observe that when using pristine MWCNTs as immobilization support the *RRA* values increase until an immobilization time of 60 min for all the materials studied, except for MWCNT-10, where the best *RRA* was found for a contact time of 30 min. Nevertheless, when the adsorption is performed onto f-MWCNTs, 30 min seems to be enough to attain the highest *RRA* values of immobilized ASNase, showing that it is not necessary to leave the enzyme in contact with the functionalized support for more time, reducing the overall processing time and costs consequently. It is worth noting that, for all cases, the *RRA* increased after MWCNTs

functionalization, indicating the importance of this step for the efficiency of the biocatalytic process, promoting larger surface areas, as was already verified. It must be noted that the best results have been achieved with the f-MWCNT-1020 reaching almost 90% of *RRA* at the end of 30 min. These results open prospects for modifying the biocompatibility of MWCNTs by varying their size and surface by chemical modification.

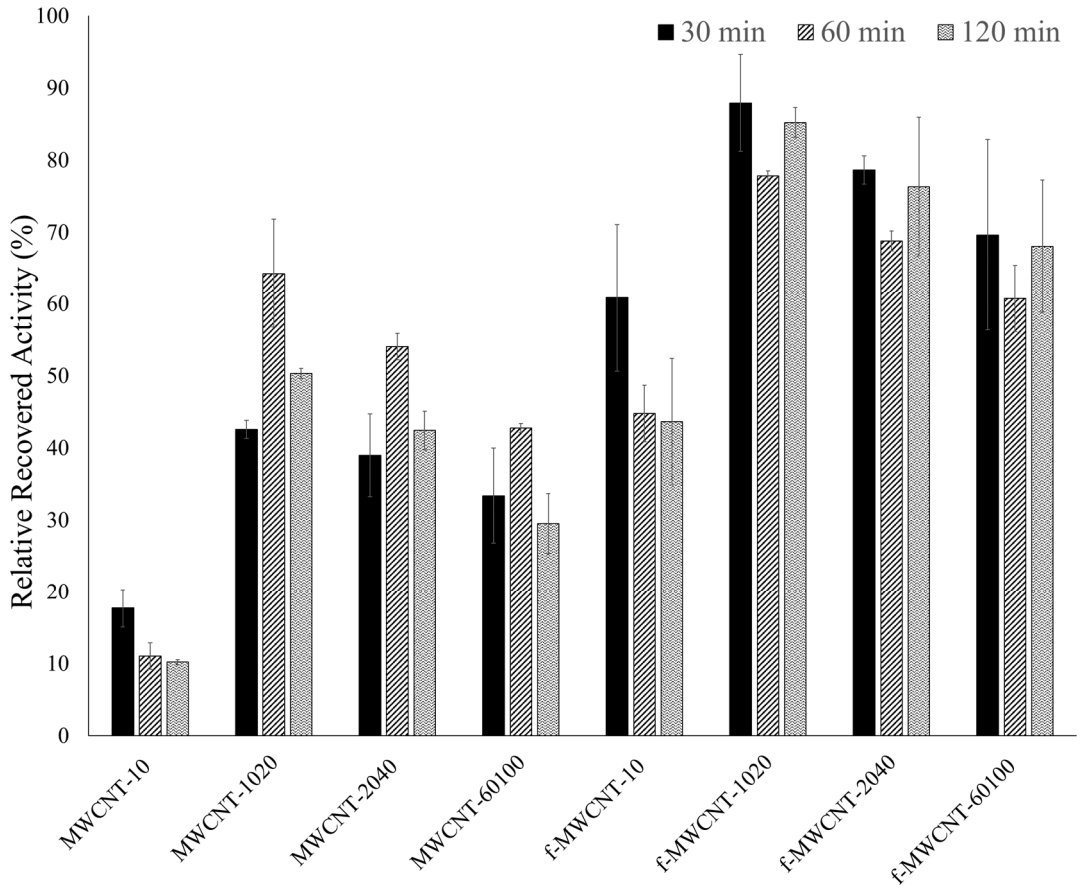

Figure 3. Effect of immobilization time and diameter of multi-walled carbon nanotubes (MWCNTs) on the relative recovered activity (*RRA*). Immobilization of 0.086 mg/mL of L-asparaginase (ASNase) onto 2 mg of pristine multi-walled carbon nanotubes (MWCNTs) and functionalized MWCNTs (f-MWCNTs) at pH 8. Error bars correspond to the standard deviation between replicates.

Once again, very high *IY* values (above 96%) were attained for all the studied samples with a contact time of only 30 min, reaching values of 100% after 120 min of immobilization time also practically for almost all the MWCNTs (Figure S2 in the Supporting Information), meaning that the enzyme is totally adsorbed.

Due to the high *RRA* and *IY* yields attained, it seems that in general, the enzyme-to-MWCNT mass ratio used is close to the maximum enzyme adsorption capacity of most of the f-MWCNTs used; however, this ratio was optimized as described below.

3.5. Effect of Enzyme Concentration on ASNase Immobilization onto MWCNTs

The analysis of the enzyme concentration to be immobilized is essential since it allows to know the maximum amount of enzyme that the support can adsorb. Different tests were conducted with varying ASNase concentrations, ranging from 0.05 to 0.6 mg/mL when immobilized onto 2 mg of pristine MWCNTs at pH 8.0 during 60 min of contact time and from 0.1 to 0.7 mg/mL when immobilized onto 2 mg of f-MWCNTs, at pH 8.0 during 30 min of contact time. In Figures 4 and 5 are visible an increment in the *RRA* with the increase in the ASNase concentration up to a particular value for all the tested MWCNTs. This behavior is due to the higher amount of ASNase molecules available to adsorb onto MWCNTs

surface. From that ASNase concentration value, a plateau is reached where the *RRA* value no longer increases with the increase in the enzyme concentration, suggesting that the MWCNTs surface attained its maximum adsorption capacity. The ASNase concentration where the *RRA* plateau is reached is considered the optimal concentration to be used in the immobilization process. Figures 4 and 5 also show almost total adsorption of ASNase onto all MWCNTs studied, with *IY* close to 100%, mainly until reaching the optimal enzyme concentration. After that concentration, there was a slight decrease in the *IY* value in some situations due to the high amount of non-adsorbed ASNase after the saturation of the support. Tang et al. [43] reported a reduction in enzyme activity at high concentrations, suggesting that this might be attributed to the hiding of certain active sites induced by enzyme aggregation. Furthermore, Li et al. [44] demonstrated that increasing enzyme concentration might also cause mass transfer blockage owing to congested space.

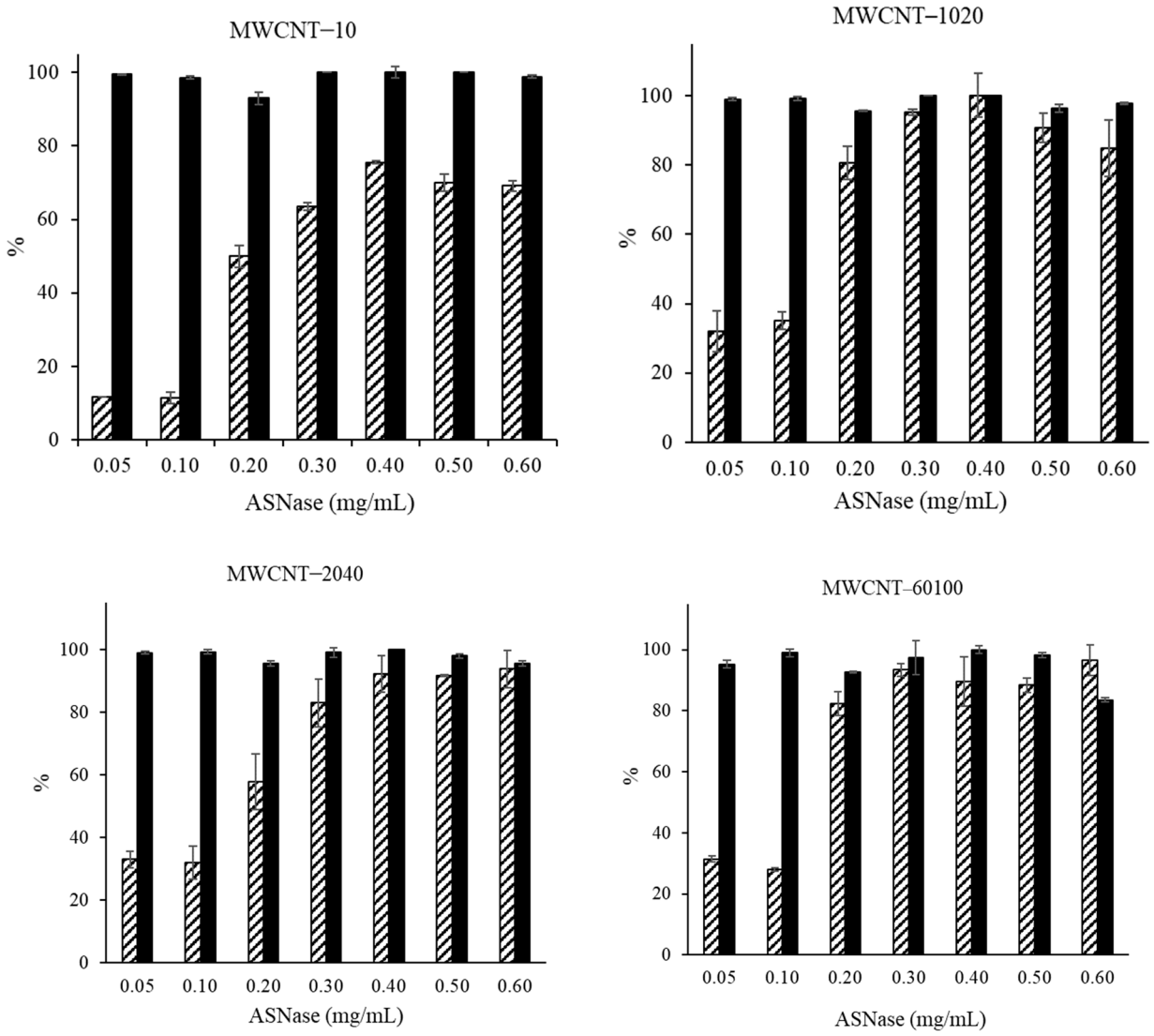

Figure 4. Effect of L-asparaginase (ASNase) concentration on the immobilization yield (*IY*) (■) and relative recovered activity (*RRA*) (▨). ASNase immobilization onto 2 mg of pristine multi-walled carbon nanotubes (MWCNTs) at pH 8.0 for 60 min. Error bars correspond to the standard deviation between replicates.

The best *RRA* and *IY* values were obtained with MWCNTs with diameters between 10 to 20 nm and 20 to 40 nm for both pristine and f-MWCNTs (Figures 4 and 5). However, note that the results are very similar for the different diameters studied. The slightly poor results for MWCNTs with diameters below 10 nm may be due to the very small

pore size, hindering the ASNase adsorption. When pristine MWCNTs with diameters of 60–100 nm were used, a certain agglomeration of the support particles was observed due to their hydrophobicity, leaving part of the support surface inaccessible, potentially affecting the attained results. One more time, the balance between the *RRA* and *IY* values attained was more favorable for the f-MWCNTs, making them the preferable support for the immobilization of ASNase.

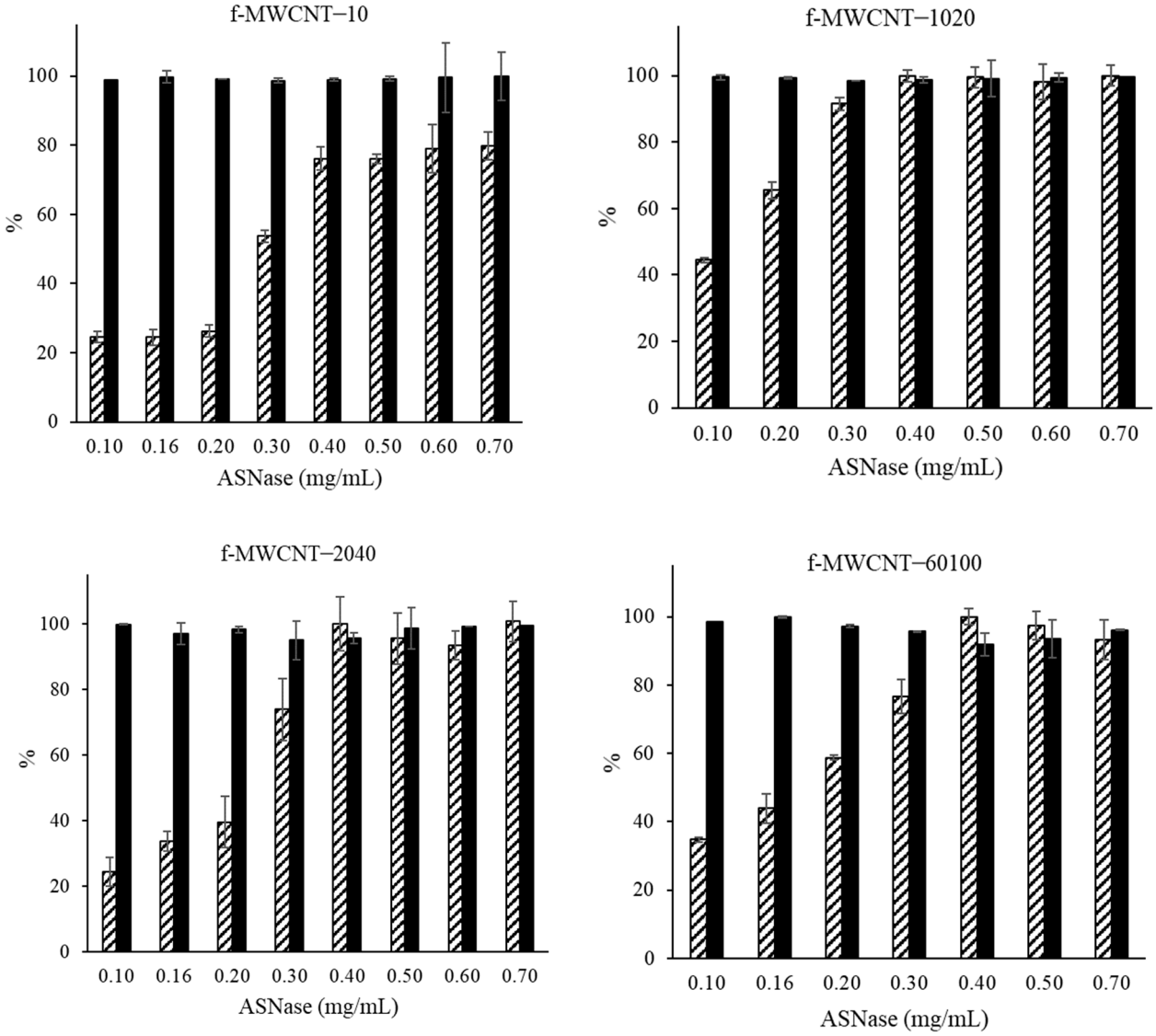

Figure 5. Effect of L-asparaginase (ASNase) concentration on the immobilization yield (*IY*) (■) and relative recovered activity (*RRA*) (▨). ASNase immobilization onto 2 mg of functionalized multi-walled carbon nanotubes (f-MWCNTs) at pH 8.0 for 30 min. Error bars correspond to the standard deviation between replicates.

ASNase immobilization on MWCNTs has already been described in the literature (Table 3). Haroun et al. [21] studied f-MWCNTs as a carrier for an ASNase from *Aspergillus versicolor* and found that physical adsorption yielded greater *IY* values (54.4%) than covalent binding, with a retained ASNase activity of 100%. The immobilization of ASNase has also been reported for other different supports, for example, Bahreini et al. [45] described an immobilized ASNase on chitosan-tripolyphosphate nanoparticles with an entrapment efficiency of around 72%. Agrawal et al. [46] showed a maximum *IY* of 85% after optimizing the covalent ASNase immobilization on aluminum oxide pellets using response surface methodology. Golestaneh & Varshosaz [47] obtained values of *IY* 95% on

silica nanoparticles using 1-ethyl-3-(3-dimethylaminopropyl) carbodiimide HCl (EDC) and glutaraldehyde as crosslinkers. These findings demonstrate the improved ability to use the f-MWCNTs of this work as support for ASNase immobilization, attaining *RRA* of 100% and *IY* of 99% without needing additional crosslinkers.

Table 3. Comparison of immobilization yield (*IY*) and relative recovered activity (*RRA*) values reported in the literature on L-asparaginase (ASNase) immobilization with those obtained in this work.

Organism Source	Immobilization Support	Immobilization Method	*IY*	*RRA*	Ref
Aspergillus versicolor	f-MWCNTs	Physical adsorption	54%	100%	[46]
E. coli	chitosan-tripolyphosphate nanoparticles	Entrapment	-	72%	[47]
E. coli	aluminum oxide pellets	Covalent linkage	85%	-	[48]
E. coli	silica nanoparticles	Cross-linkage	95%	-	[49]
E. coli	f-MWCNTs	Physical adsorption	99%	100%	This work

3.6. Operational Stability

The enzyme reusability is vital from the commercial point of view since it enables process costs reduction. The immobilization of ASNase enables enzyme recovery and reuse after each reaction. Six L-asparagine hydrolysis cycles were performed to assess the reusability of the ASNase immobilized onto pristine and f-MWCNTs-1020 (as one of the best-determined diameters) at the optimal conditions, by analysis of *RRA*, where the first cycle's *RRA* was established as 100%. After six continuous reaction cycles, the ASNase immobilized onto pristine MWCNTs retained 57 ± 8% of its initial activity (Figure 6a). The supernatant solution was analyzed via the enzyme activity method at the end of each cycle, indicating almost no active ASNase leakage in the supernatant solutions. Therefore, the reduction in the enzymatic activity might be related to the deactivation of the immobilized enzyme. When immobilized onto f-MWCNTs, the ASNase could be reused at least six times without losing significant activity, maintaining 74 ± 2% of its initial activity (Figure 6b). The MWCNTs functionalization provides a stronger linkage between the enzyme and the support, preventing the ASNase denaturation. The slight decrease in activity seen after repeated use could be due to active site deformation caused by frequent interactions among L-asparagine and the active site of the immobilized ASNase.

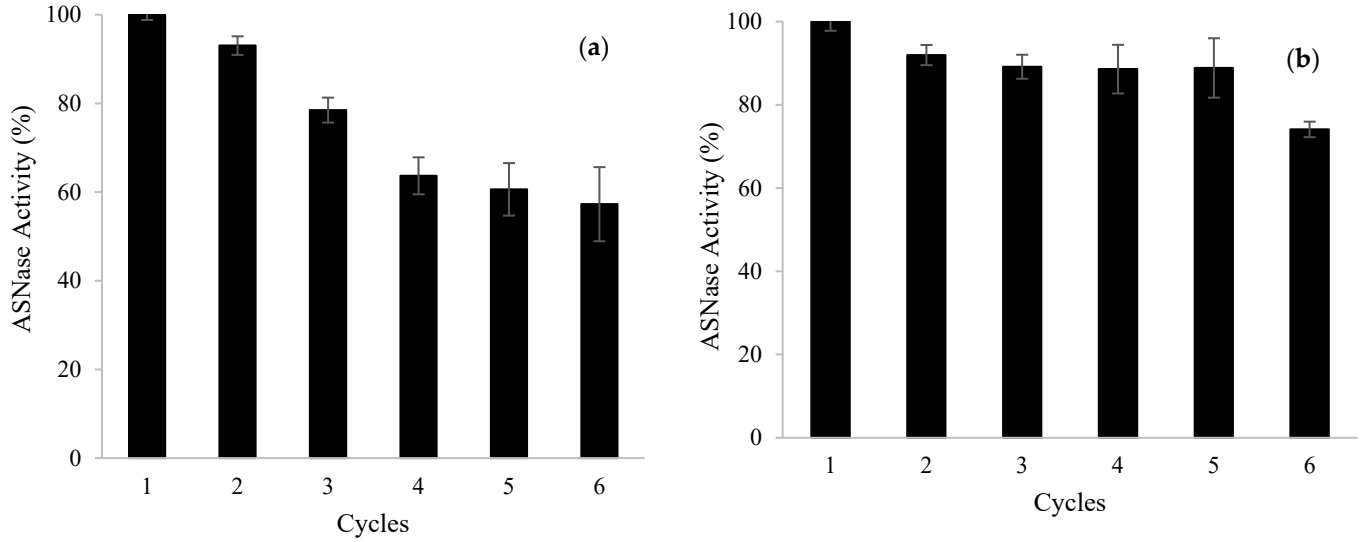

Figure 6. Operational stability of immobilized L-asparaginase (ASNase) onto (**a**) pristine and (**b**) functionalized multi-walled carbon nanotubes (f-MWCNTs-1020). Error bars correspond to the standard deviation between replicates.

Ulu [48] reported similar operational stability of ASNase immobilized onto metal-organic frameworks. The enzyme retained roughly 78% of its original activity after five cycles. Furthermore, after ten cycles, approximately 45% of the original activity was preserved. These results can also be compared with the ones obtained by Noma et al. [49] using poly (2-hydroxyethyl methacrylate-glycidyl methacrylate) cryogels as enzyme carriers, where ASNase was able to retain 52% after ten cycles. These results highlight the suitability of the ASNase immobilization onto f-MWCNTs employed in this study to maintain equivalent enzyme activity and avoid considerable enzyme leaching due to desorption during continuous usage.

3.7. Kinetic Parameters Determination

Changing the L-asparagine concentration through the hydrolytic reaction made it possible to investigate the kinetics of free and immobilized ASNase onto pristine and f-MWCNTs. Figure 7 depicts the sigmoidal dependence of the ASNase enzymatic reaction rate on L-asparagine concentration, which is typical of allosteric enzymes. This kinetic behavior is described by the Hill Equation (Equation (1)) [16], and Figure 7 proves the excellent fit of experimental data to this allosteric sigmoidal model. Although Hill's model for the immobilized enzyme was assumed, in these cases it is important to consider that the mathematic interpretation of reaction–diffusion equations for immobilized catalyzers is much more complex [50]. In fact, the "apparent constants" are highly dependent on the working conditions (e.g., the use of rotating electrodes are essential for mass transport, diffusion and solution stirring can modify the real concentration at the enzyme layer, immobilization protocol leads to steric hindrance or claimed multilayers, etc.) [51].

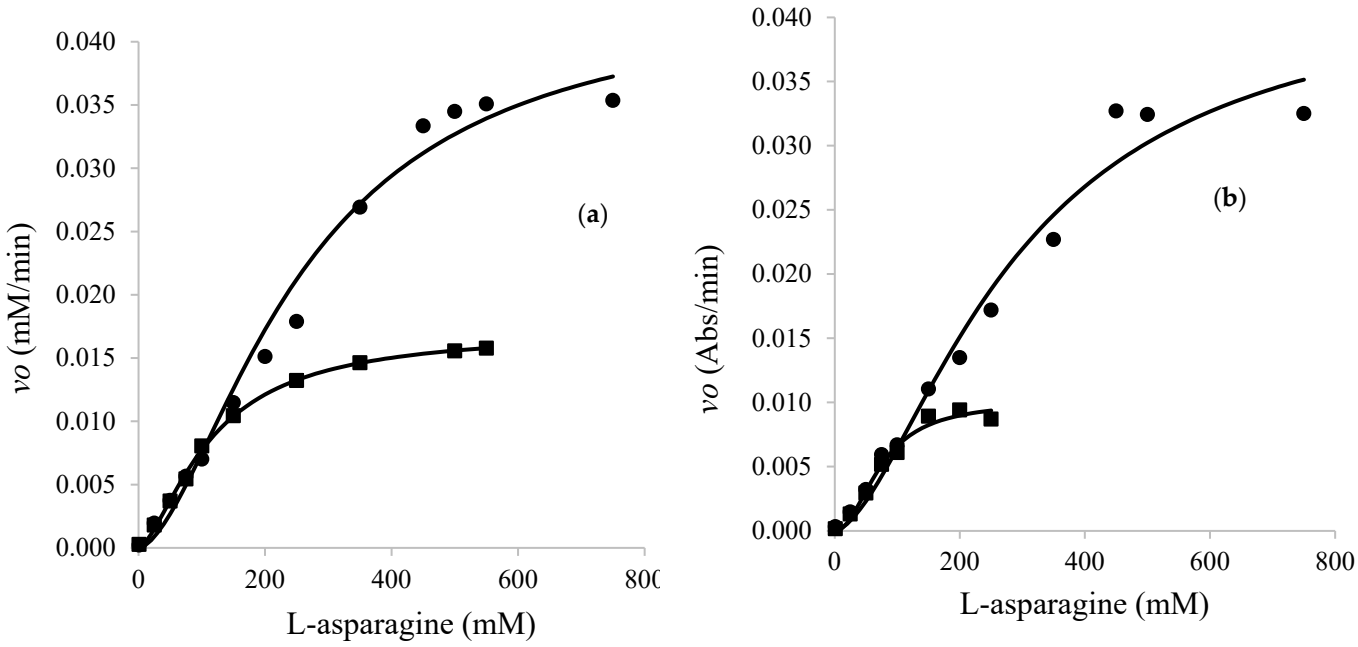

Figure 7. Initial reaction rates (v_0) for both (•) free and (■) immobilized L-asparaginase (ASNase) onto (**a**) pristine and (**b**) functionalized multi-walled carbon nanotubes (f-MWCNTs-1020) by physical adsorption. The solid lines represent the experimental data fit to the Hill equation.

Table 4 summarizes the kinetic properties of free ASNase and both types of ASNase-MWCNT bioconjugate, also presenting the resultant catalytic efficiencies (k_{cat}/S_{50}). The S_{50} values for 0.3 and 0.4 mg/mL of free ASNase were 288 and 258 mM, respectively; nevertheless, a reduction in these values was noted when analyzing the immobilized ASNase: 114 and 74 mM, when pristine and f-MWCNTs were used, respectively. The reduction confirmed in S_{50} for the ASNase-MWCNT complex, similar to the Michaelis-Menten constant (K_M), indicates that the affinity of the enzyme for the substrate improved

as a consequence of immobilization, hence enhancing its activity. The ASNase particle may be stretched over the MWCNTs surface with better positioning, resulting in increased active site availability and improved affinity for L-asparagine [52]. Through evaluation of S_{50} for the immobilized enzyme, it was also possible to verify an improved affinity to the substrate when using f-MWCNTs as support. The determination of S_{50} values also allowed to verify that the use of 189 nm of L-asparagine for the ASNase activity measurement, as reported in the literature [53], was well applied in the case of free ASNase. For the immobilized ASNase lower L-asparagine concentrations could have been used, but it would not allow us to make the intended comparisons. In addition, reported concentration of L-asparagine in leukemia blood serum samples varies from 10^{-3} to 10^{-2} M, while in healthy blood serum samples varies from 10^{-6} to 10^{-4} M [7,54,55].

Table 4. Kinetic parameters for free and immobilized L-asparaginase (ASNase) onto pristine and functionalized multi-walled carbon nanotubes (f-MWCNTs).

	MWCNT		f-MWCNT	
	Free ASNase (0.3 mg/mL)	**Immobilized ASNase**	**Free ASNase (0.4 mg/mL)**	**Immobilized ASNase**
v_{max} **(mM min^{-1})**	0.044	0.017	0.043	0.010
S_{50} **(mM)**	258.0	113.6	288.3	73.8
h	1.7	1.6	1.6	2.1
k_{cat}/S_{50} **(mM^{-1} min^{-1})**	4.65	1.83	3.40	0.81

A 2.6-fold reduction on v_{max} values from 0.044 to 0.017 mM·min^{-1} was observed comparing free and immobilized ASNase onto pristine MWCNTs. This decrease was even more pronounced when immobilizing 0.4 mg/mL of ASNase onto f-MWCNTs, with a 4.3-fold decrease in the v_{max} value. The lower v_{max} detected after immobilization is due to the diffusion layer around ASNase molecules exhibiting a more significant mass transfer limitation [56], hindering the diffusion of L-asparagine in the direction of ASNase-MWCNTs bioconjugate. The immobilization of enzymes can also decrease molecular flexibility, which is often reflected in an inferior catalytic activity [56] and, subsequently, in a fall in v_{max} value upon immobilization. When paralleled to the ASNase free form, these kinetic constants resulted in lower catalytic efficiencies (k_{cat}/S_{50}) of immobilized ASNase (Table 4) due to changes in its three-dimensional structure resulting from the adsorption to a solid support and the consequent steric hindrance. In addition to the lower catalytic efficiency, the immobilized enzyme showed a higher affinity for the substrate and it is important to take into account the good reusability presented by the immobilized ASNase, thus proving that carbon nanotubes are a good matrix for immobilization of this enzyme Analogous results were reported by Ulu et al. [5] and Orhan and Uygun [57] where the v_{max} of immobilized ASNase was also lower than that of free ASNase and the enzyme affinity towards its substrate also increased after immobilization.

The Hill coefficient, n, represents the degree of cooperation among the enzyme subunits and the substrate molecules number that can attach to the enzyme complex. Equation (1) is simplified to the Michaelis-Menten equation when n equals 1. Positive cooperativity (homotropic regulation) is indicated by a value of $n > 1$, which means numerous substrate molecules attach to the enzyme concurrently. A value of $n < 1$ shows negative cooperativity; the attachment or catalysis of the second substrate molecule is hampered by the first's binding. In this study, the determined Hill coefficient values above 1 (Table 4) indicate that both free and immobilized ASNase forms have allosteric regulation with positive cooperativity.

4. Conclusions

The immobilization of ASNase onto pristine and f-MWCNTs with different size diameters proved to affect the properties of the ASNase bioconjugate. The hydrothermal treatment with nitric acid promoted a higher specific surface area of the material due to

the creation of defect sites and holes on the sidewalls of the tubes, improving the support capacity to bind more enzyme particles and, consequently, to achieve higher enzyme *RRA*. In turn, the best *RRA* results of adsorbed ASNase were obtained with f-MWCNTs-1020 and f-MWCNTs-2040, showing the importance of the nanomaterial diameter size for the enzyme binding. MWCNTs with diameters smaller than 10 nm showed to be too small for total enzyme binding, even presenting larger specific surface areas. MWCNTs with diameters larger than 40 nm revealed lower ASNase activity after immobilization, probably due to the smaller surface areas and, consequently, fewer ASNase molecules adsorbed.

The optimization of the immobilization conditions made it possible to attain *RRA* and *IY* values of 100 and 99%, respectively, when immobilizing 0.4 mg/mL of ASNase onto 2 mg of f-MWCNTs-1020 during 30 min of contact time, at pH 8. The calculation of the ASNase *pI* (5.2) together with the determination of the pH_{PZC} of the f-MWCNTs (3–4) showed that under the optimal conditions, the primary binding forces responsible for the ASNase adsorption onto f-MWCNTs are most likely π-π, CH-π and hydrophobic interactions.

Exceptional operational stability was achieved when immobilizing the ASNase onto f-MWCNTs, allowing its reuse for six reaction cycles with a retained activity of 74 ± 2%, value 1.3 times higher than when immobilized onto pristine MWCNTs (57 ± 8%). Determining the kinetic parameters for this allosteric enzyme also proved that the immobilization onto MWCNTs improved the ASNase affinity for the substrate, especially when using the functionalized materials.

This work demonstrates the impact of MWCNTs diameter and surface functionalization on the binding of ASNase and biocompatibility of the bioconjugate, maximizing their potential application in the pharmaceutical, food or biosensing industries.

Supplementary Materials: The following supporting information can be downloaded at: https://www.mdpi.com/article/10.3390/app12178924/s1, Figure S1. Effect of pH and diameter of multi-walled carbon nanotubes (MWCNTs) on the immobilization yield (*IY*). Immobilization of 0.086 mg/mL of L-asparaginase (ASNase) onto 2 mg of pristine (MWCNTs) and functionalized MWCNTs (f-MWCNTs) for 60 min of contact time. Error bars correspond to the standard deviation between replicates. Figure S2. Effect of immobilization time and diameter of multi-walled carbon nanotubes (MWCNTs) on the immobilization yield (*IY*). Immobilization of 0.086 mg/mL of L-asparaginase (ASNase) onto 2 mg of pristine (MWCNTs) and functionalized MWCNTs (f-MWCNTs) at pH 8. Error bars correspond to the standard deviation between replicates.

Author Contributions: R.O.C., J.G.P., L.S.T. and M.C.N.: methodology, investigation. R.O.C. and R.A.M.B.: writing—original draft. M.G.F., J.L.F., V.C.S.-E., A.P.M.T. and C.G.S.: methodology, investigation, funding acquisition, resources, writing—review and editing. R.O.C., A.P.M.T. and C.G.S.: supervision. All authors have read and agreed to the published version of the manuscript.

Funding: This work was financially supported by: LA/P/0045/2020 (ALiCE) and UIDB/50020/2020–UIDP/50020/2020 (LSRE-LCM) funded by national funds through FCT/MCTES (PIDDAC), and POCI-01-0145-FEDER-031268 funded by FEDER, through COMPETE2020-Programa Operacional Competitividade e Internacionalização (POCI), and by national funds (OE), through FCT/MCTES. This work was developed within the scope of the project CICECO-Aveiro Institute of Materials, UIDB/50011/2020, UIDP/50011/2020 & LA/P/0006/2020, financed by national funds through FCT/MEC (PIDDAC). This work was also supported by São Paulo Research Foundation (FAPESP)–Brazil [Grant no. FAPESP 2018/06908-8].

Data Availability Statement: The datasets used and/or analyzed during the current study are available from the corresponding author/s at reasonable request.

Acknowledgments: V.C.S.-E. thanks the National Council of Scientific and Technological Development, Brazil (Conselho Nacional de Desenvolvimento Científico e Tecnológico—CNPq) and the fellowships from CNPq (grant no. 312463/2021-9). M.C.N. and A.P.M.T. acknowledge FCT for the research contracts CEECIND/00383/2017 and CEECIND/2020/01867, respectively.

Conflicts of Interest: The authors declare no conflict of interest.

References

1. Jozala, A.F.; Geraldes, D.C.; Tundisi, L.L.; Feitosa, V.A.; Breyer, C.A.; Cardoso, S.L.; Mazzola, P.G.; Oliveira-Nascimento, L.; Rangel-Yagui, C.O.; Magalhães, P.O.; et al. Biopharmaceuticals from microorganisms: From production to purification. *Braz. J. Microbiol. Publ. Braz. Soc. Microbiol.* **2016**, *47* (Suppl. 1), 51–63. [CrossRef] [PubMed]
2. Panke, S.; Wubbolts, M.G. Enzyme technology and bioprocess engineering. *Curr. Opin. Biotechnol.* **2002**, *13*, 111–116. [CrossRef]
3. Miranda-Filho, A.; Piñeros, M.; Ferlay, J.; Soerjomataram, I.; Monnereau, A.; Bray, F. Epidemiological patterns of leukaemia in 184 countries: A population-based study. *Lancet. Haematol.* **2018**, *5*, e14–e24. [CrossRef] [PubMed]
4. Zhang, Y.-Q.; Tao, M.-L.; Shen, W.-D.; Zhou, Y.-Z.; Ding, Y.; Ma, Y.; Zhou, W.-L. Immobilization of l-asparaginase on the microparticles of the natural silk sericin protein and its characters. *Biomaterials* **2004**, *25*, 3751–3759. [CrossRef] [PubMed]
5. Ulu, A.; Ates, B. Immobilization of l-Asparaginase on Carrier Materials: A Comprehensive Review. *Bioconjug. Chem.* **2017**, *28*, 1598–1610. [CrossRef]
6. Aiswarya, R.; Baskar, G. Enzymatic mitigation of acrylamide in fried potato chips using asparaginase from Aspergillus terreus. *Int. J. Food Sci. Technol.* **2018**, *53*, 491–498.
7. Nunes, J.C.F.; Cristóvão, R.O.; Freire, M.G.; Santos-Ebinuma, V.C.; Faria, J.L.; Silva, C.G.; Tavares, A.P.M. Recent Strategies and Applications for l-Asparaginase Confinement. *Molecules* **2020**, *25*, 5827. [CrossRef]
8. Haroun, A.; Mostafa, H.; Ahmed, E. Functionalized Multi-walled Carbon Nanotubes as Emerging Carrier for Biological Applications. In Proceedings of the 5th World Congress on New Technologies (NewTech'19), Lisbon, Portugal, 18–20 August 2019.
9. Cristóvão, R.O.; Almeida, M.R.; Barros, M.A.; Nunes, J.C.F.; Boaventura, R.A.R.; Loureiro, J.M.; Faria, J.L.; Neves, M.C.; Freire, M.G.; Ebinuma-Santos, V.C.; et al. Development and characterization of a novel l-asparaginase/MWCNT nanobioconjugate. *RSC Adv.* **2020**, *10*, 31205–31213. [CrossRef]
10. Verma, S.K.; Modi, A.; Bellare, J. Polyethersulfone-carbon nanotubes composite hollow fiber membranes with improved biocompatibility for bioartificial liver. *Colloids Surf. B Biointerfaces* **2019**, *181*, 890–895.
11. Zhao, X.; Tian, K.; Zhou, T.; Jia, X.; Li, J.; Liu, P. PEGylated multi-walled carbon nanotubes as versatile vector for tumor-specific intracellular triggered release with enhanced anti-cancer efficiency: Optimization of length and PEGylation degree. *Colloids Surfaces B Biointerfaces* **2018**, *168*, 43–49. [CrossRef]
12. Costa, J.B.; Lima, M.J.; Sampaio, M.J.; Neves, M.C.; Faria, J.L.; Morales-Torres, S.; Tavares, A.P.M.; Silva, C.G. Enhanced biocatalytic sustainability of laccase by immobilization on functionalized carbon nanotubes/polysulfone membranes. *Chem. Eng. J.* **2019**, *355*, 974–985. [CrossRef]
13. Mohamad, N.R.; Marzuki, N.H.C.; Buang, N.A.; Huyop, F.; Wahab, R.A. An overview of technologies for immobilization of enzymes and surface analysis techniques for immobilized enzymes. *Biotechnol. Biotechnol. Equip.* **2015**, *29*, 205–220. [CrossRef] [PubMed]
14. Wang, J.; Liu, G.; Lin, Y. Amperometric choline biosensor fabricated through electrostatic assembly of bienzyme/polyelectrolyte hybrid layers on carbon nanotubes. *Analyst* **2006**, *131*, 477–483. [CrossRef] [PubMed]
15. Silva, C.G.; Tavares, A.P.M.; Dražić, G.; Silva, A.M.T.; Loureiro, J.M.; Faria, J.L. Controlling the Surface Chemistry of Multiwalled Carbon Nanotubes for the Production of Highly Efficient and Stable Laccase-Based Biocatalysts. *ChemPlusChem* **2014**, *79*, 1116–1122. [CrossRef]
16. Elena, V.E. Graphical Approach to Compare Concentration Constants of Hill and Michaelis-Menten Equations. *J. Biotechnol. Biomed. Sci.* **2018**, *1*, 94–99.
17. Zhou, Y.; Fang, Y.; Ramasamy, R.P. Non-Covalent Functionalization of Carbon Nanotubes for Electrochemical Biosensor Development. *Sensors* **2019**, *19*, 392. [CrossRef]
18. Hu, C.-Y.; Xu, Y.-J.; Duo, S.-W.; Zhang, R.-F.; Li, M.-S. Non-Covalent Functionalization of Carbon Nanotubes with Surfactants and Polymers. *J. Chin. Chem. Soc.* **2009**, *56*, 234–239. [CrossRef]
19. Ali Mohammadi, Z.; Aghamiri, S.F.; Zarrabi, A.; Talaie, M.R. A comparative study on non-covalent functionalization of carbon nanotubes by chitosan and its derivatives for delivery of doxorubicin. *Chem. Phys. Lett.* **2015**, *642*, 22–28. [CrossRef]
20. Ulu, A.; Karaman, M.; Yapıcı, F.; Naz, M.; Sayın, S.; Saygılı, E.İ.; Ateş, B. The Carboxylated Multi-walled Carbon Nanotubes/l-Asparaginase Doped Calcium-Alginate Beads: Structural and Biocatalytic Characterization. *Catal. Lett.* **2020**, *150*, 1679–1691. [CrossRef]
21. Haroun, A.A.A.; Ahmed, H.M.; Mossa, A.; Mohafrash, S.M.M.; Ahmed, E.F. Production, characterization and immobilization of Aspergillus versicolor L-asparaginase onto multi-walled carbon nanotubes. *Biointerface Res. Appl. Chem.* **2020**, *10*, 733740.
22. Almeida, M.R.; Cristóvão, R.O.; Barros, M.A.; Nunes, J.C.F.; Boaventura, R.A.R.; Loureiro, J.M.; Faria, J.L.; Neves, M.C.; Freire, M.G.; Santos-Ebinuma, V.C.; et al. Superior operational stability of immobilized l-asparaginase over surface-modified carbon nanotubes. *Sci. Rep.* **2021**, *11*, 21529. [CrossRef] [PubMed]
23. Zhao, X.; Lu, D.; Hao, F.; Liu, R. Exploring the diameter and surface dependent conformational changes in carbon nanotube-protein corona and the related cytotoxicity. *J. Hazard. Mater.* **2015**, *292*, 98–107. [CrossRef] [PubMed]
24. Mu, Q.; Liu, W.; Xing, Y.; Zhou, H.; Li, Z.; Zhang, Y.; Ji, L.; Wang, F.; Si, Z.; Zhang, B.; et al. Protein Binding by Functionalized Multiwalled Carbon Nanotubes Is Governed by the Surface Chemistry of Both Parties and the Nanotube Diameter. *J. Phys. Chem. C* **2008**, *112*, 3300–3307. [CrossRef]
25. Rivera-Utrilla, J.; Bautista-Toledo, I.; Ferro-García, M.A.; Moreno-Castilla, C. Activated carbon surface modifications by adsorption of bacteria and their effect on aqueous lead adsorption. *J. Chem. Technol. Biotechnol.* **2001**, *76*, 1209–1215. [CrossRef]

26. Marques, R.; Machado, B.; Faria, J.; Silva, A. Controlled generation of oxygen functionalities on the surface of Single-Walled Carbon Nanotubes by HNO_3 hydrothermal oxidation. *Carbon* **2010**, *48*, 1515–1523. [CrossRef]
27. Barros, R.A.M.; Cristóvão, R.O.; Carabineiro, S.A.C.; Neves, M.C.; Freire, M.G.; Faria, J.L.; Santos-Ebinuma, V.C.; Tavares, A.P.M.; Silva, C.G. Immobilization and Characterization of L-Asparaginase over Carbon Xerogels. *BioTech* **2022**, *11*, 10. [CrossRef]
28. Walters, D.E. *Enzymes A: Practical Introduction to Structure, Mechanism, and Data Analysis*, 2nd ed.; Copeland, R.A., Ed.; Wiley-VCH: New York, NY, USA, 2000; pp. xvi, 397. ISBN 0-471-35929-7.
29. Feng, W.; Ji, P. Enzymes immobilized on carbon nanotubes. *Biotechnol. Adv.* **2011**, *29*, 889–895. [CrossRef]
30. Shim, M.; Shi Kam, N.W.; Chen, R.J.; Li, Y.; Dai, H. Functionalization of Carbon Nanotubes for Biocompatibility and Biomolecular Recognition. *Nano Lett.* **2002**, *2*, 285–288. [CrossRef]
31. Wang, L.; Wei, L.; Chen, Y.; Jiang, R. Specific and reversible immobilization of NADH oxidase on functionalized carbon nanotubes. *J. Biotechnol.* **2010**, *150*, 57–63. [CrossRef]
32. Hou, J.; Xu, L.; Han, Y.; Tang, Y.; Wan, H.; Xu, Z.; Zheng, S. Deactivation and regeneration of carbon nanotubes and nitrogen-doped carbon nanotubes in catalytic peroxymonosulfate activation for phenol degradation: Variation of surface functionalities. *RSC Adv.* **2019**, *9*, 974–983. [CrossRef]
33. Peigney, A.; Laurent, C.; Flahaut, E.; Bacsa, R.R.; Rousset, A. Specific surface area of carbon nanotubes and bundles of carbon nanotubes. *Carbon* **2001**, *39*, 507–514. [CrossRef]
34. Chen, M.; Yu, H.-W.; Chen, J.-H.; Koo, H.-S. Effect of purification treatment on adsorption characteristics of carbon nanotubes. *Diam. Relat. Mater.* **2007**, *16*, 1110–1115. [CrossRef]
35. Lemes, A.P.; Montanheiro, T.L.d.A.; da Silva, A.P.; Durán, N. PHBV/MWCNT Films: Hydrophobicity, Thermal and Mechanical Properties as a Function of MWCNT Concentration. *J. Compos. Sci.* **2019**, *3*, 12. [CrossRef]
36. Amaral Montanheiro, T.L.; Montagna, L.S.; Machado, J.P.B.; Lemes, A.P. Covalent functionalization of MWCNT with PHBV chains: Evaluation of the functionalization and production of nanocomposites. *Polym. Compos.* **2019**, *40*, 288–295. [CrossRef]
37. Salgin, S.; Salgin, U.; Bahadir, S. Zeta Potentials and Isoelectric Points of Biomolecules: The Effects of Ion Types and Ionic Strengths. *Int. J. Electrochem. Sci.* **2012**, *7*, 12404–12414.
38. Bae, N.; Pollak, A.; Lubec, G. Proteins from Erwinia asparaginase Erwinase® and *E. coli* asparaginase 2 MEDAC® for treatment of human leukemia, show a multitude of modifications for which the consequences are completely unclear. *Electrophoresis* **2011**, *32*, 1824–1828. [CrossRef]
39. Liu, Y.; Pietzsch, M.; Ulrich, J. Purification of L-asparaginase II by crystallization. *Front. Chem. Sci. Eng.* **2013**, *7*, 37–42. [CrossRef]
40. Zhu, J.H.; Yan, X.L.; Chen, H.J.; Wang, Z.H. In situ extraction of intracellular L-asparaginase using thermoseparating aqueous two-phase systems. *J. Chromatogr. A* **2007**, *1147*, 127–134. [CrossRef]
41. Noma, S.A.A.; Ulu, A.; Acet, Ö.; Sanz, R.; Sanz-Pérez, E.S.; Odabaşı, M.; Ateş, B. Comparative study of ASNase immobilization on tannic acid-modified magnetic Fe_3O_4/SBA-15 nanoparticles to enhance stability and reusability. *New J. Chem.* **2020**, *44*, 4440–4451. [CrossRef]
42. Verma, S.; Mehta, R.K.; Maiti, P.; Röhm, K.H.; Sonawane, A. Improvement of stability and enzymatic activity by site-directed mutagenesis of *E. coli* asparaginase II. *Biochim. Et Biophys. Acta* **2014**, *1844*, 1219–1230. [CrossRef] [PubMed]
43. Tang, T.; Fan, H.; Ai, S.; Han, R.; Qiu, Y. Hemoglobin (Hb) immobilized on amino-modified magnetic nanoparticles for the catalytic removal of bisphenol A. *Chemosphere* **2011**, *83*, 255–264. [CrossRef]
44. Li, P.; Ma, X.-H.; Dong, Y.-M.; Jin, L.; Chen, J. α-Glucosidase immobilization on polydopamine-coated cellulose filter paper and enzyme inhibitor screening. *Anal. Biochem.* **2020**, *605*, 113832. [CrossRef] [PubMed]
45. Bahreini, E.; Aghaiypour, K.; Abbasalipourkabir, R.; Mokarram, A.R.; Goodarzi, M.T.; Saidijam, M. Preparation and nanoencapsulation of l-asparaginase II in chitosan-tripolyphosphate nanoparticles and in vitro release study. *Nanoscale Res. Lett.* **2014**, *9*, 340. [CrossRef] [PubMed]
46. Agrawal, S.; Sharma, I.; Prajapati, B.P.; Suryawanshi, R.K.; Kango, N. Catalytic characteristics and application of l-asparaginase immobilized on aluminum oxide pellets. *Int. J. Biol. Macromol.* **2018**, *114*, 504–511. [CrossRef]
47. Golestaneh, D.; Varshosaz, J. Enhancement in Biological Activity of L-Asparginase by its Conjugation on Silica Nanoparticles. *Recent Pat. Nanotechnol.* **2018**, *12*, 70–82. [CrossRef]
48. Ulu, A. Metal–organic frameworks (MOFs): A novel support platform for ASNase immobilization. *J. Mater. Sci.* **2020**, *55*, 6130–6144. [CrossRef]
49. Ali Noma, S.A.; Acet, Ö.; Ulu, A.; Önal, B.; Odabaşı, M.; Ateş, B. l-asparaginase immobilized p(HEMA-GMA) cryogels: A recent study for biochemical, thermodynamic and kinetic parameters. *Polym. Test.* **2021**, *93*, 106980. [CrossRef]
50. Silverstein, T.P.; Goodney, D.E. Enzyme-Linked Biosensors: Michaelis−Menten Kinetics Need Not Apply. *J. Chem. Educ.* **2010**, *87*, 905–907. [CrossRef]
51. Valencia, P.; Ibañez, F. Estimation of the Effectiveness Factor for Immobilized Enzyme Catalysts through a Simple Conversion Assay. *Catalysts* **2019**, *9*, 930. [CrossRef]
52. Hosseinipour, S.L.; Khiabani, M.S.; Hamishehkar, H.; Salehi, R. Enhanced stability and catalytic activity of immobilized α-amylase on modified Fe_3O_4 nanoparticles for potential application in food industries. *J. Nanopart. Res.* **2015**, *17*, 382. [CrossRef]
53. Magri, A.; Soler, M.F.; Lopes, A.M.; Cilli, E.M.; Barber, P.S.; Pessoa, A., Jr.; Pereira, J.F.B. A critical analysis of L-asparaginase activity quantification methods-colorimetric methods versus high-performance liquid chromatography. *Anal. Bioanal. Chem.* **2018**, *410*, 6985–6990. [CrossRef] [PubMed]

54. Nunes, J.C.F.; Cristóvão, R.O.; Santos-Ebinuma, V.C.; Faria, J.L.; Silva, C.G.; Neves, M.C.; Freire, M.G.; Tavares, A.P.M. L-Asparaginase-Based Biosensors. *Encyclopedia* **2021**, *1*, 848–858. [CrossRef]
55. Tundisi, L.L.; Coêlho, D.F.; Zanchetta, B.; Moriel, P.; Pessoa, A.; Tambourgi, E.B.; Silveira, E.; Mazzola, P.G. L-Asparaginase Purification. *Sep. Purif. Rev.* **2017**, *46*, 35–43. [CrossRef]
56. Gashtasbi, F.; Ahmadian, G.; Noghabi, K.A. New insights into the effectiveness of alpha-amylase enzyme presentation on the Bacillus subtilis spore surface by adsorption and covalent immobilization. *Enzym. Microb. Technol.* **2014**, *64–65*, 17–23. [CrossRef]
57. Orhan, H.; Aktaş Uygun, D. Immobilization of L-Asparaginase on Magnetic Nanoparticles for Cancer Treatment. *Appl. Biochem. Biotechnol.* **2020**, *191*, 1432–1443. [CrossRef]